doi：103969/j. issn. 0490-6756. 2016. 11. 019

理论研究不对称团簇$(HFBN_3)_n$(n=1－6)的结构和稳定性

马登学，夏其英，高志梅
(临沂大学化学化工学院，临沂 276000)

摘　要：采用密度泛函理论方法研究不对称团簇$(HFBN_3)_n$(n=1－6)的结构和性质. 对于 $n\geqslant 2$ 的团簇，B-N_α 键易形成，而 B-B 和 N_α-N_α 键不存在. 讨论了几何参数随团簇尺寸 n 的变化规律. 通过分析团簇平均结合能和二阶差分值，探讨其相对稳定性，发现团簇$(HFBN_3)_3$ 比其它团簇更稳定. 计算 IR 谱有四个特征区. 研究了团簇的热力学性质随温度 T 以及团簇尺寸 n 的变化趋势. 室温下，由焓变可知单体 1 形成多聚体(2、3、4、5、6)在热力学上有利.

关键词：$(HFBN_3)_n$(n=1－6)；密度泛函理论(DFT)；IR 谱
中图分类号：O64　　**文献标识码**：A　　**文章编号**：0490-6756(2016)06-1299-08

Theoretical investigation of structures and stabilities for asymmetric clusters $(HFBN_3)_n$(n=1－6)

MA Deng-Xue, *XIA Qi-Ying*, *GAO Zhi-Mei*
(School of Chemistry and Chemical Engineering, Linyi University, Linyi 276005, China)

Abstract: Density functional theory has been applied to investigate the structures and properties of asymmetric clusters $(HFBN_3)_n$(n=1－6). When $n\geqslant 2$, B-N_α bonds form easily, and B-B and N_α-N_α bonds are not found in the clusters. The geometric parameters of clusters along with cluster size n are discussed. The relative stabilities of asymmetric clusters $(HFBN_3)_n$(n=1－6) are analyzed based on the averaged binding energy and second-order difference of energy. It is found that $(HFBN_3)_3$ clusters are more stable than other clusters. The calculated IR spectra have four main characteristic regions. Trends in thermodynamic properties with temperature T and cluster size n are discussed, respectively. Monomer 1 forms clusters (2, 3, 4, 5 and 6) thermodynamically favorable by the enthalpies at 298.2 K.

Keywords: Asymmetric clusters $(HFBN_3)_n$(n=1－6); Density functional theory (DFT); IR spectra

1　Introduction

Wiberg and Michaud reported the synthesis of the first azide of the element boron $B(N_3)_3$ in 1954 [1], which undergoes a spontaneous gas-phase decomposition to produce BN films at room temperature [2]. The chemistry of boron azides, including $(CH_3)_2BN_3$, $(n\text{-}C_3H_7)_2BN_3 \cdot Py$, $(n\text{-}C_4H_9)_2BN_3$, $(X_2BN_3)_3$ (X = F, Cl, Br), and $[(C_6F_5)_2BN_3]_{2-3}$ etc [3-9], was further investigated and reviewed by Paetzold, Fraenk and co-workers. It is well known that all of the mono-

收稿日期：2016-05-16
基金项目：国家自然科学基金(21203086)；山东省自然科学基金(ZR2012BL09)
作者简介：马登学(1976－)，男，山东临沂人，副教授，主要研究领域为计算化学.
通讯作者：夏其英. E-mail：xiaqiying@163.com

meric liquid or solid boron azides were reported in the literature except for the trimeric boron dihalide azides $(X_2BN_3)_3$(X= F, Cl, Br) and dimethylboron azide showing a temperature dependent oligomerization [3,4]. The extensive studies on boron azides are motivated by the fact that these molecules have been shown to be good single source precursors (SSP) for boron nitride (BN) film deposition. Despite the extensive experimental studies in the condensed phase, experimental data for the gas phase species are rare and knowledge of their gas phase stability and thermodynamic properties becomes essential. Previous theoretical studies of the boron azides were reported on the symmetric boron azides [10,11]. Here, motivated by and based on previously experimental studies on asymmetric clusters of gallium azides and aluminum azides $(RR'MN_3)_n$(M=Al, Ga; R $=CH_3$, H; R'=Cl, Br; $n=3-4$) [12,13], we choose the simple model for the inorganic asymmetric boron azide compounds $(HFBN_3)_n$(n=1−6) to study. To the best of our knowledge, there are no structural data for the asymmetric clusters $(HFBN_3)_n$(n=1−6) in the literature, neither experimental nor theoretical in nature. The aim of this paper is a detailed theoretical investigation of structural, stability, IR spectra and thermodynamic characteristics of the asymmetric clusters $(HFBN_3)_n$(n=1−6), which may provide some useful information for the subsequent experimental studies.

2 Computational methods

All calculations reported in this study were performed using the Gaussian 09 suite of programs [14]. The initial structure of the cluster was constructed manually, taking previous investigations into consideration. A number of initial structural guesses were generated, and the corresponding geometries were then optimized using B3LYP method with the 6−31G * basis set [15,16]. Final optimizations were performed under tight conditions, with no integral symmetry imposed. Frequencies along with their respective IR intensities were then calculated, and the lack of imaginary frequencies confirmed in each case that a true minimum was obtained.

3 Results and discussion

3.1 Structures

The most stable structures of each size for the asymmetric clusters $(HFBN_3)_n$(n=1−6) optimized at the B3LYP/6−31G * level are illustrated in Fig. 1. Table 1 depicts the ranges of geometrical parameters and energies for corresponding structures. Two stably structures with C_1 symmetry$_f$or monomer $HFBN_3$ were obtained (Fig. 1, 1, connectivity: HFB-N_α-N_β-N_γ). Two dimers, ten trimers, fifty three tetramers, two hundred and fifty-six pentamers and five hundred and forty-seven hexamers are obtained. After n≥2, all the structures are cyclic with an alternation of B and N_α atoms, which is in line with the results reported in the previous literatures [10,11]. From Fig. 1, one can see B-N_α bonds form easily, and B-B and N_α-N_α bonds are not found in the clusters. Judged by the total energies, the most stable isomers of each size are labeled as 1, 2, 3, 4, 5 and 6.

For monomer $HFBN_3$, the azide group is slight bent with a N_α-N_β-N_γ angle of 172.9°. The B-N_α bond length (0.1436 nm) is between that of a B-N single (0.158 nm) and double bond (0.137 nm). The N_β-N_γ bond length (0.1135 nm) is shorter than the N_α-$N_\beta$bond (0.1239 nm). N_α-N_β and N_β-$N_\gamma$bond lengths are close to a N-N double (0.125 nm) and a N-N triple bond (0.110 nm), respectively. From $n=2$, the computed B-N_α bonds (0.1588-0.1643 nm) have typical B-N single bond character. These B-N_α are still considerably longer than those found for four-coordinate boron in the reported tetrazidoborate anion $[B(N_3)_4]^-$ which shows B-N_3 bond lengths of 0.1542(8) nm (X-ray, average) [7], and are comparable with the bond lengths of other covalent boron azides previously determined, such as $(Cl_2BN_3)_3$(0.158nm),

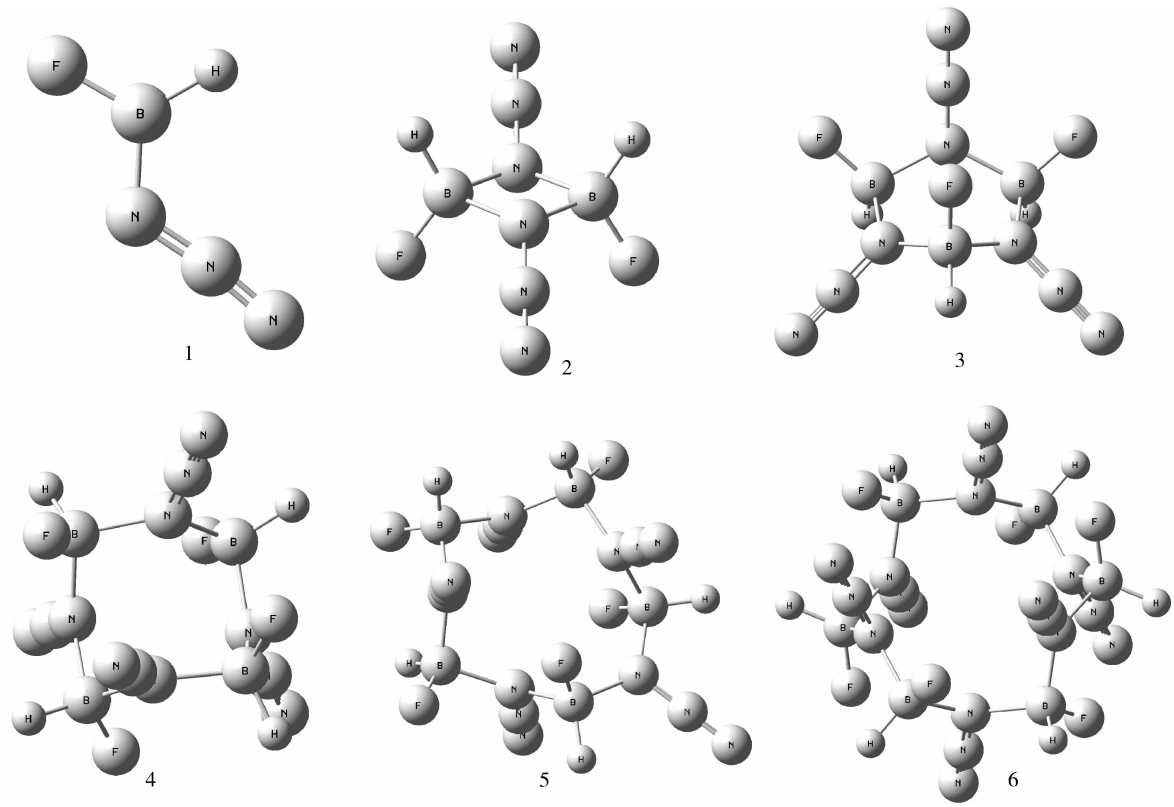

Fig. 1　The most stable structures for the asymmetric clusters $(HFBN_3)_n$(n=1－6)

$(F_2BN_3)_3$(0.1616 nm) and $(C_6F_5B(N_3)_2)_3$(0.160 nm)[6, 9]. For $n=2-6$, the B-H and B-F bond lengths outside the ring are in the range of 0.1199－0.1202 nm and 0.1354－0.1378 nm, respectively. The computed structural parameters for the azide units for $n\geqslant 2$ are 0.1242－0.1257 nm for N_α-N_β bonds and 0.1126－0.1131 nm for N_β-N_γ bonds with N_α-N_β-N_γ bond angles of 176.8－180.0°. Again, those values are in excellent agreement with the corresponding bond lengths in $(Cl_2BN_3)_3$ (0.125 nm, 0.109 nm, 178°), $(F_2BN_3)_3$(0.1249 nm, 0.1129 nm, 179.8°) and $(C_6F_5B(N_3)_2)_3$(0.127 nm, 0.111 nm, 179°)[6, 9]. The very good agreement between our calculated values and the experimental ones is a validation of the reliability of the present calculation.

Tab. 1　Ranges of the bond lengths, bond angles, and energies for the most stable structures of the asymmetric clusters $(HFBN_3)_n$(n=1－6)

	1	2	3	4	5	6
rN_β-N_γ/nm	0.1135	0.1131	0.1126－0.1130	0.1129	0.1127－0.1130	0.1128
rN_α-N_β/nm	0.1239	0.1242－0.1243	0.1245－0.1257	0.1250	0.1249－0.1255	0.1253
rB-H/nm	0.1194	0.1199	0.1200－0.1202	0.1200	0.1198－0.1202	0.1199
rB-N_α/nm	0.1436	0.1631	0.1594－0.1637	0.1588－0.1635	0.1589－0.1643	0.1592－0.1640
rB-F/nm	0.1323	0.1354	0.1369－0.1367	0.1375	0.1368－0.1375	0.1378
θN_α-N_β-N_γ/°	172.9	176.8－177.3	176.9－179.1	178.8	178.8－180.0	178.6
θN_β-N_α-B/°	120.8	122.9－124.2	116.3－118.3	115.8－117.2	114.8－117.6	117.4
θB-N_α-B/°		93.9－94.3	123.9－124.4	127.0	124.9－128.3	124.5
θN_α-B-N_α/°		85.9	100.8－102.2	104.0	105.3－106.7	106.8－106.9
E/kJ·mol^{-1}	－760275.81	－1520559.45	－2280917.88	－3041237.54	－3801549.59	－4561856.62
E_b/kJ·mol^{-1}		7.83	90.45	134.3	170.54	201.76
ZPE/kJ·mol^{-1}	76.76	160.87	247.03	331.79	415.65	498.89
E_{b-c}/kJ·mol^{-1}		0.77	74.37	110.54	139.96	164.96
$E_{b-c-ave}$/kJ·mol^{-1}		0.39	24.79	27.63	27.99	27.49

Moreover, the cluster size n has important influences on the geometries. The average B-N_α bond distance increases with n increasing, but this change is not monotonic, and when $n=5-6$, the increase of B-N_α bond length is not obvious. As may be seen from Table 1, the B-F bond lengths exhibit a similar trend as the cyclic clusters enlarge. When $n=1-3$, the N_α-N_β and B-H bond lengths increases, and when $n=4-6$, the changes of those bond lengths are slight. The value of the N_β-N_γ bond lengths decreases from 0.1135 nm in 1 to 0.1128 nm in 6, and then tend to be constant at around 0.1128 nm with $n=3-6$. Compared with monomer 1, the increasing bond lengths of N_α-N_β, B-H and B-F outside of the rings showed it could easily eliminate N_2(N_β-N_γ), H_2 and F^- groups to yield BN material. The bond angles of N_α-B-N_α and B-N_α-B increase as the cyclic clusters size n increases, while N_β-N_α-B bond angles decrease except for 6. The B-N_α-B bond angles in the cyclic clusters are consistently larger than N_α-B-N_α bond angles.

3.2 Energetic Properties

For the following oligomerization processes

$$n\mathrm{HFBN_3} \rightarrow (\mathrm{HFBN_3})_n (n=2-6)$$

the uncorrected binding energies (E_b), corrected binding energies (E_{b-c}), average corrected binding energy ($E_{b-c-ave}$), and the second-order energy difference ($\Delta_2 E$) are calculated using the following formulas:

$$E_b(n)=nE(\mathrm{HFBN_3})-E(\mathrm{HFBN_3})_n \quad (1)$$

$$E_{b-c}(n)=n*E(\mathrm{HFBN_3})+0.96*n*ZPE(\mathrm{HFBN_3})-E(\mathrm{HFBN_3})_n-0.96*ZPE(\mathrm{HFBN_3})_n \quad (2)$$

$$E_{b-c-ave}(n)=E_{b-c}(n)/n \quad (3)$$

$$\Delta_2 E(n)=E(\mathrm{HFBN_3})_{n+1}+0.96*ZPE(\mathrm{HFBN_3})_{n+1}+E(\mathrm{HFBN_3})_{n-1}+0.96*ZPE(\mathrm{HFBN_3})_{n-1}-2*E(\mathrm{HFBN_3})_n-2*0.96*ZPE(\mathrm{HFBN_3})_n \quad (4)$$

where $E(\mathrm{HFBN_3})_n$ and $E(\mathrm{HFBN_3})$ are the total energies of the most stable structures for clusters $(\mathrm{HFBN_3})_n$ ($n=2-6$) and $\mathrm{HFBN_3}$, respectively; $ZPE(\mathrm{HFBN_3})_n$ and $ZPE(\mathrm{HFBN_3})$ are the zero point energies of the most stable structures for clusters $(\mathrm{HFBN_3})_n$ ($n=2-6$) and $\mathrm{HFBN_3}$, respectively. The scaling factor is 0.96 [17].

From Table 1, one can see that the proportions of ZPE corrections to their binding energies E_b are large, which indicates it is necessary to carry out the ZPE corrections for the binding energies. With cluster size n increasing, the E_b and E_{b-c} values generally increase, which imply that the clusters can continue to gain energy during the growth process. As shown in Fig. 2 (a), the $E_{b-c-ave}$ quickly increase as the clusters size grows for $n\leqslant 3$. For $n=4-6$, $E_{b-c-ave}$ slowly increase as the cluster size grows, then tend to be constant at around 28 kJ·mol^{-1}. Which shows that the cluster size ($n=4-6$) has little effect on the average corrected binding energies. The second-order energy difference ($\Delta_2 E$) is one sensitive parameter that reflects the relative stabilities of clusters. From Fig. 2 (b), one can see the local peak appear at the size of $n=3$, implying that the cluster $(\mathrm{HFBN_3})_3$ has higher stability than their vicinal clusters.

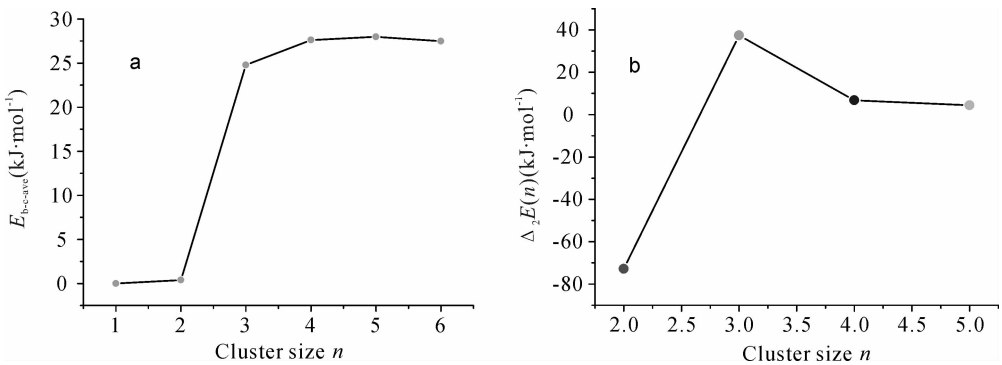

Fig. 2 $E_{b-c-ave}$ (a) and $\Delta_2 E$ (b) of the asymmetric clusters $(\mathrm{HFBN_3})_n$ ($n=1-6$) as a function of cluster size n

3.3 IR Spectrum

IR spectrum is not only the basic property of compounds, but also an effective measure to identify substances. Besides, it has a direct relation with the thermodynamic properties. Fig. 3 presents the IR spectra of the clusters $(HFBN_3)_n$(n=1－6) simulated at the B3LYP/6－31＊ level, in which vibrational frequencies have been scaled by a factor 0.96 to remove the systematic overestimation [17]. Fig. 3 shows that there are four main characteristic regions associated with the B-H stretching vibration, asymmetric and symmetric stretching of N_3, and the fingerprint region in the lower frequencies. Usually, as the atomic mass increases, the corresponding vibrational frequency shifts toward the lower wavenumber. Since the mass of the hydrogen atom is the smallest, the B－H stretching vibrations occur at the higher region of approximately 2500 cm^{-1}. As the number of B－H bonds increases from 1 to 5, the vibrational modes of B-H shift to the lower wavenumber (a red shift), and no obvious shift is observed for n=5－6. The mode of 2220－2252 cm^{-1} in the most stable asymmetric clusters $(HFBN_3)_n$(n=1－6), which is consistent with that found for boron dichloride azide $(Cl_2BN_3)_3$ (2210 cm^{-1}) and $[(C_6F_5)_2BN_3]_2$ (2202 cm^{-1}) [6, 9], corresponds to the N_3 asymmetric stretching vibration. The N_3 asymmetric stretching vibration shows a blue shift with an increase in size from 1 to 6. The following modes are in the ranges of 1234－1391 cm^{-1} corresponding to the N_3 symmetric stretching vibration. These N_3 symmetric stretching frequencies generally reveal a red shift with gradual increase of cluster size. The fingerprint region, at less than 1187 cm^{-1}, mainly involves stretching of rings, the stretching of B-F, the wagging and scissoring of H-B-F, and the N_3 deformation vibrations, which is used to identify isomers. Meanwhile, in three characteristic regions with N_3 asymmetric, N_3 symmetric and B-H stretching vibration, the number of vibration equals to that of azido groups and B-H bonds, respectively.

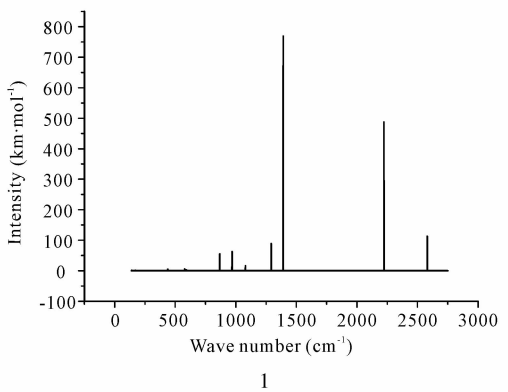

1

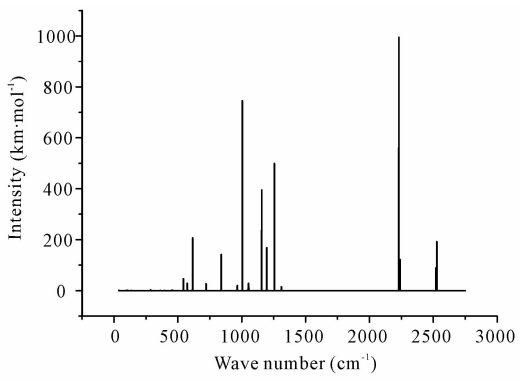

2

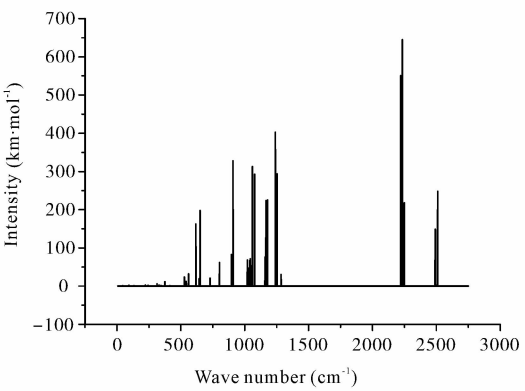

3

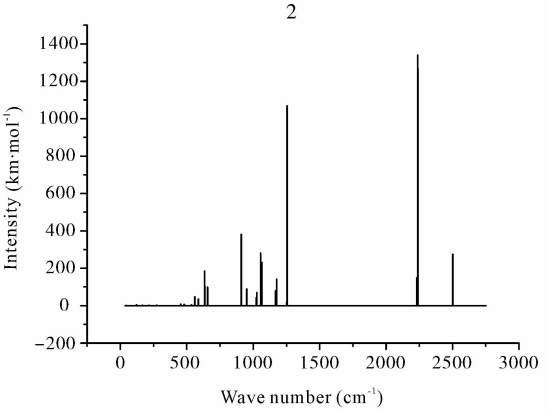

4

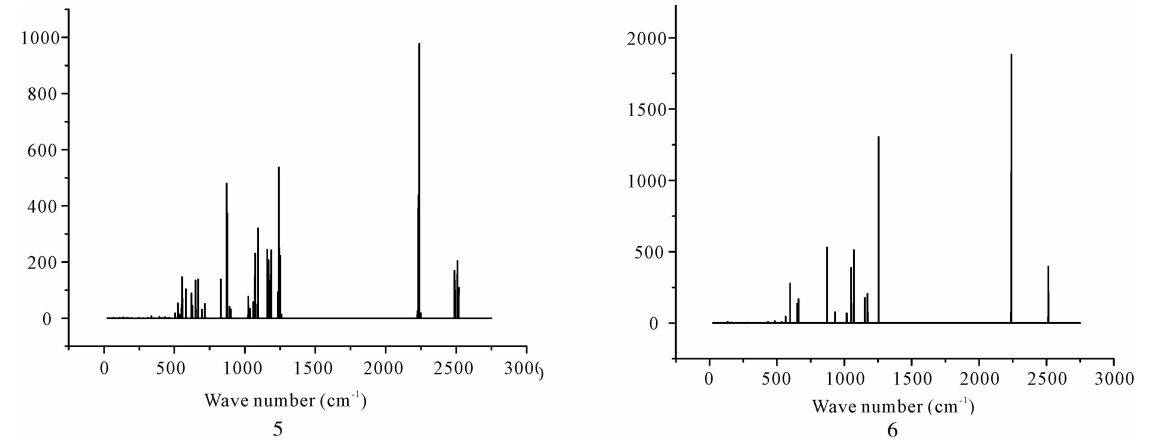

Fig. 3 IR spectra for the most stable clusters $(HFBN_3)_n$ (n=1−6)

3.4 Thermodynamic Properties

On the basis of vibrational analysis and statistical thermodynamic method, the thermodynamic functions including heat capacity ($C^{\theta}_{p,m}$), entropy (S^{θ}_{m}), and enthalpy (H^{θ}_{m}) for the most stable isomers of the asymmetric clusters $(HFBN_3)_n$ (n=1−6) ranging from 200 to 800 K are evaluated and presented in Table 2. Firstly, as can be seen, thermodynamic functions of the asymmetric clusters $(HFBN_3)_n$ (n=1−6) all increase evidently as the temperature increases. This is because the main contributions to the thermodynamic functions are from the translations and rotations of the molecules at lower temperature, whereas the vibrational motion is intensified at higher temperature and makes more contributions to the thermodynamic functions. For intuitive illustration, monomer 1 was taken from the title compounds as typical examples to show the temperature−dependent relationships for $C^{\theta}_{p,m}$, S^{θ}_{m}, and H^{θ}_{m}, which has been presented in Fig. 4(a). It is obvious that as the temperature increases, the increments for $C^{\theta}_{p,m}$ and S^{θ}_{m} both decrease but that H^{θ}_{m} increases constantly. However, since the coefficients of T^2 are very small, these correlations are approximate to linear equations. In other words, thermodynamic functions of monomer 1 increase linearly with the temperature on the whole. This hold true for the other asymmetric clusters $(HFBN_3)_n$ (n=2−6).

Tab. 2 Thermodynamic properties for the most stable structure of the asymmetric clusters $(HFBN_3)_n$ (n=1−6) at different temperatures

cluster	T/K	200	298.2	400	500	600	700	800
1	$C^{\theta}_{p,m}$/ J·mol^{-1}·K^{-1}	57.97	70.22	81.21	89.93	96.90	102.51	107.05
	S^{θ}_{m}/ J·mol^{-1}·K^{-1}	269.73	295.19	317.41	336.51	353.54	368.91	382.91
	H^{θ}_{m}/ kJ·mol^{-1}	8.95	15.25	22.98	31.55	40.91	50.89	61.37
2	$C^{\theta}_{p,m}$/ J·mol^{-1}·K^{-1}	115.45	148.61	175.28	194.98	210.02	221.76	231.10
	S^{θ}_{m}/ J·mol^{-1}·K^{-1}	360.52	413.03	460.61	501.94	538.88	572.17	602.41
	H^{θ}_{m}/ kJ·mol^{-1}	15.09	28.11	44.67	63.22	83.51	105.12	127.78
3	$C^{\theta}_{p,m}$/ J·mol^{-1}·K^{-1}	174.72	225.56	266.82	297.43	320.81	339.03	353.48
	S^{θ}_{m}/ J·mol^{-1}·K^{-1}	458.08	537.67	610.00	672.98	729.37	780.24	826.49
	H^{θ}_{m}/ kJ·mol^{-1}	22.04	41.77	66.94	95.23	126.19	159.22	193.87
4	$C^{\theta}_{p,m}$/ J·mol^{-1}·K^{-1}	236.56	305.22	360.62	401.63	432.93	457.29	476.60
	S^{θ}_{m}/ J·mol^{-1}·K^{-1}	519.22	626.98	724.79	809.87	885.99	954.63	1017.00
	H^{θ}_{m}/ kJ·mol^{-1}	28.83	55.55	89.58	127.79	169.59	214.15	260.88
5	$C^{\theta}_{p,m}$/ J·mol^{-1}·K^{-1}	299.62	385.44	454.69	506.00	545.17	575.67	599.84
	S^{θ}_{m}/ J·mol^{-1}·K^{-1}	598.39	734.65	858.06	965.30	1061.17	1147.59	1226.10
	H^{θ}_{m}/ kJ·mol^{-1}	36.09	69.87	112.82	160.97	213.61	269.72	328.54
6	$C^{\theta}_{p,m}$/ J·mol^{-1}·K^{-1}	362.41	466.42	549.77	610.89	656.91	692.25	719.88
	S^{θ}_{m}/ J·mol^{-1}·K^{-1}	681.99	846.86	996.16	1125.73	1241.36	1345.39	1439.70
	H^{θ}_{m}/ kJ·mol^{-1}	43.23	84.10	136.05	194.23	257.73	325.26	395.92

On the other hand, with the increase in the number of cluster size n, thermodynamic functions of the most stable asymmetric clusters $(HFBN_3)_n$(n=2－6) all increase monotonically at 298.2 K, as shown in Fig. 4(b). The contribution of monomer $HFBN_3$ to the thermodynamic properties matches the cluster additivity. Each monomer $HFBN_3$ contributes to the $C^{\theta}_{p,m}$, S^{θ}_{m}, and H^{θ}_{m} by 79 J·mol^{-1}·K^{-1}, 109 J·mol^{-1}·K^{-1}, and 14 kJ·mol^{-1}, respectively.

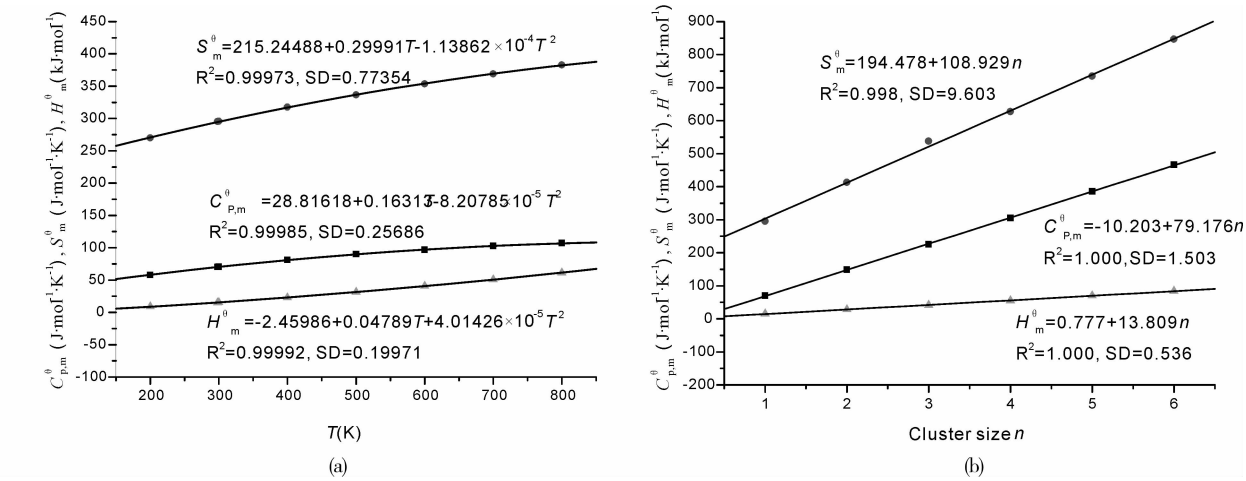

Fig. 4　Evolution of the thermodynamic functions with the temperature (T) (a) and the cluster size n (b) for the asymmetric clusters $(HFBN_3)_n$(n=1－6)

The values of theoretical enthalpies (ΔH) and Gibbs free energies (ΔG) in the processes of 1→2, 3, 4, 5, and 6 at temperatures of 200－800 K can be found in Table 3. The values of ΔH in the processes are negative except for 1→2 in 600－800 K, which reveals that these oligomerizations are exothermic. The values of ΔG are positive at 298.2 K, which indicates the oligomerizations can not occur spontaneously.

Tab. 3　Oligomerization enthalpies and Gibbs free energies at different temperatures

progress	T/K	200	298.2	400	500	600	700	800
2(1)→2	ΔH/ kJ·mol^{-1}	−3.58	−3.16	−2.06	−0.65	0.92	2.57	4.27
	ΔG/ kJ·mol^{-1}	32.20	49.72	67.62	84.89	101.84	118.52	134.99
3(1)→3	ΔH/ kJ·mol^{-1}	−79.18	−78.35	−76.37	−73.79	−70.91	−67.82	−64.61
	ΔG/ kJ·mol^{-1}	−8.96	25.39	60.52	94.49	127.84	160.72	193.18
4(1)→4	ΔH/ kJ·mol^{-1}	−117.51	−115.99	−112.88	−108.95	−104.59	−99.95	−95.14
	ΔG/ kJ·mol^{-1}	−5.57	49.15	105.06	159.14	212.31	264.76	316.57
5(1)→5	ΔH/ kJ·mol^{-1}	−148.62	−146.34	−142.04	−136.74	−130.90	−124.69	−118.27
	ΔG/ kJ·mol^{-1}	1.43	74.71	149.55	221.88	293.01	363.18	432.49
6(1)→6	ΔH/ kJ·mol^{-1}	−175.43	−172.36	−166.79	−160.03	−152.69	−145.04	−137.26
	ΔG/ kJ·mol^{-1}	11.84	103.26	196.53	286.63	375.23	462.61	548.94

4　Conclusions

The structural feature, energies, IR spectra, and thermodynamic properties of the asymmetric clusters $(HFBN_3)_n$(n=1－6) have been calculated at the B3LYP/6－31G* level. Results show that the asymmetric clusters $(HFBN_3)_n$(n=2－6) contain $(BN)_{2n}$ cyclic structures. The relationships between geometrical parameters and cluster size n are discussed. The binding energies E_b and E_{b-c} reveal that the asymmetric clusters $(HFBN_3)_n$(n=1－6) can continue to gain energy as n increasing. The calculated second－order difference in

energy ($\Delta_2 E$) suggest that the cluster $(HFBN_3)_3$ are relatively stable. There are four main characteristic regions in the IR spectra, which are associated with the B—H stretching vibration, the N_3 symmetric and asymmetric stretching vibrations, and the ? ngerprint region. As the cluster size n increases, the B-H stretching vibrations and the N_3 symmetric stretching motion shift to the lower wavenumbers, while the N_3 asymmetric stretching motion moves to a higher region. Thermodynamic functions ($C^{\theta}_{p,m}$, S^{θ}_{m} and H^{θ}_{m}) for $(HFBN_3)_n$ (n=1—6) clusters all increase linearly with the increasing temperature T and cluster size n. Judged by the enthalpies at 298.2 K, all the oligomerizations are thermodynamically favorable.

References:

[1] Wiberg E, Michaud H. Pentafluorophenyl and phenyl substituted azidoborates [J]. Z Naturforsch, 1954, 96: 497.

[2] Mulinax R L, Okin G S, Coombe R D. Gas phase synthesis, structure, and dissociation of boron triazide [J]. J Phys Chem, 1995, 99: 6294.

[3] Müller J, Paetzold P I. The reaction of decaborane with hydrazoic acid: A novel access to azaboranes [J]. Heteroat Chem, 1990, 1: 461.

[4] Hausser-Wallis R, Oberhammer H, Einholz W, *et al*. Gas-phase structures of dimethylboron azide and dimethylboron isocyanate. Electron diffraction and ab initio study [J]. Inorg Chem, 1990, 29: 3286.

[5] Fraenk W, Klapötke T M, Krumm B, *et al*. Bis (pentafluorophenyl) boron azide: synthesis and structural characterization of the first dimeric boron azide [J]. Chem Commun, 2000, 667.

[6] Fraenk W, Klapötke T M, Krumm B, *et al*. Oligomeric pentafluorophenylboron azides [J]. J Chem Soc, Dalton Trans, 2000, 4635.

[7] Fraenk W, Habereder T, Hammerl A, *et al*. Highly energetic tetraazidoborate anion and boron triazide adducts [J]. Inorg Chem, 2001, 40: 1334.

[8] Johnson L A, Sturgis S A, Al-Jihad I A, *et al*. Low-temperature matrix isolation and photolysis of BCl_2N_3: spectroscopic identification of the photolysis product ClBNCl [J]. J Phys Chem A, 1999, 103: 686.

[9] Fraenk W, Klapötke T M. Theoretical studies on the thermodynamic stability and trimerization of BF_2N_3 [J]. J Fluorine Chem, 2001, 111: 45.

[10] Ma D X, Xia Q Y, Zhang C. Theoretical studies on structural feature and thermodynamic stability of F_2BN_3 oligomers [J]. J At Mol Phys, 2009, 26(2): 361.

[11] Ma D X, Xia Q Y. Theoretical studies on the structures and properties of the $(H_2BN_3)_n$ (n = 1 — 4) clusters [J]. Chem Res Appl, 2009, 21(6): 852.

[12] McMurran J, Kouvetakis J, Nesting D C, *et al*. Formation of a tetrameric, cyclooctane-like, azidochlorogallane, $[HClGaN_3]_4$, and related azidogallanes. Exothermic single-source precursors to GaN nanostructures [J]. J Am Chem Soc, 1998, 120: 5233.

[13] Kouvetakis J, McMurran J, Steffek C, *et al*. Synthesis and structures of heterocyclic azidogallanes $[(CH_3)ClGaN_3]_4$ and $[(CH_3)BrGaN_3]_3$ en route to $[(CH_3)HGaN_3]_x$: an inorganic precursor to GaN [J]. Inorg Chem, 2000, 39: 3805.

[14] Frisch M J, Trucks G W, Schlegel H B, *et al*. Gaussian 09, Revision A. 02 [CP]. Wallingford CT: Gaussian, Inc, 2009.

[15] Becke A D. Density-functional thermochemistry. III. The role of exact exchange [J]. J Chem Phys, 1993, 98: 5648.

[16] Lee C, Yang W, Parr R G. Development of the Colle-Salvetti correlation-energy formula into a functional of the electron density [J]. Phys Rev B, 1988, 37: 785.

[17] Scott A P, Radom L. Harmonic vibrational frequencies: an evaluation of Hartree-Fock, MΦller-Plesset, quadratic configuration interaction, density functional theory, and semiempirical scale factors [J]. J Phys Chem, 1996, 100: 16502.